THE INFLUENCE OF THE RED SEA RIFTS AND THE GULF OF ADEN RIFTS ON THE LATERAL PROPAGATIONS OF FAULTS IN THE DOBI GRABEN AND ITS SURROUNDING AREA IN THE AFAR DEPRESSION

Zelalem Demissie. Department of Geology, Wichita State University. Wichita, Kansas *zelalem.demissie@wichita.edu * T43E-0493

ABSTRACT

The Dobi graben is a NW-trending, Quaternary continental rift found within the East-Central Block (ECB) of the Afar Depression (AD) in northeastern Ethiopia. Extension occurs on steeply dipping faults, where the ratio of maximum displacement to traced fault length extends to four orders of magnitude. We conducted fault population analysis in the Dobi graben using a 30 m resolution Shuttle Rader Topography Mission (SRTM) Digital Elevation Model (DEM). We traced a total of 953 faults. We used the fault displacement length profiles' tapering directions and the different types of the fault propagations' termination styles to characterize the fault kinematics pattern. Our population analysis results show that ~45% of the normal faults in the Dobi graben are tapering towards the southeast in a manner similar to the Red Sea Rift (RSR) regional strain gradient. On the other hand, our analysis showed that ~40% of the faults in the Dobi graben are tapering towards the northwest direction in a manner similar to the Gulf of Aden Rift (GAR) regional strain gradient. We found the statistical regression correlation coefficients (R-square value) for both the southeast and the northwest tapering faults to be ~0.7. Therefore, we suggest that ~85% of the lateral propagation of the 953 faults in the Dobi graben is highly influenced by the regional strain transfer of the RSR and GAR. Additionally, based on the fault propagation termination styles, our faults population analysis shows that faults which exhibit the half-restricted termination style account for 85% of the 953 faults. The maximum displacement over maximum length (Dmax/Lmax) ratio of these faults is 0.03, which is in accord with the constant displacement length fault growth model.

STUDY AREA

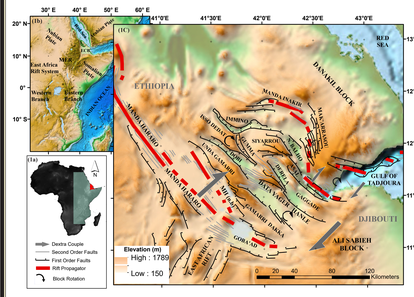

Figure 1: (A) Digital Elevation Model (DEM) of Africa. The mint color area represents the region affected by the East Africa Rift System (EARS) and the small red polygon in the Horn of Africa represents the Afar Depression (AD); (B) The EARS. The northern tip is the Ad which comprises the East Central Block (ECB) in the center. The eastern and the western branch of the EARS exist south of MER; (C) The tectonic framework of the Afar depression (AD) shown in Shuttle Radar Topographic Mission (SRTM) referred as Digital Elevation Model (DEM). Solid red lines indicate major rift propagators mainly the Red Sea Propagator (RSP) and Gulf of Aden Propagator (GAP). The element of rifts and blocks structures in the AD is represented by black lines and second-order faults with gray lines, respectively (Manighetti et al., 2001a). Clockwise rotation of the NW-trending blocks (Kidane et al., 2003) displayed with black curve arrow lines, and both NE and SW-directed dextral strike-slip shear couples are indicated with broad, gray, arrow lines.

Tectonic History and Geology

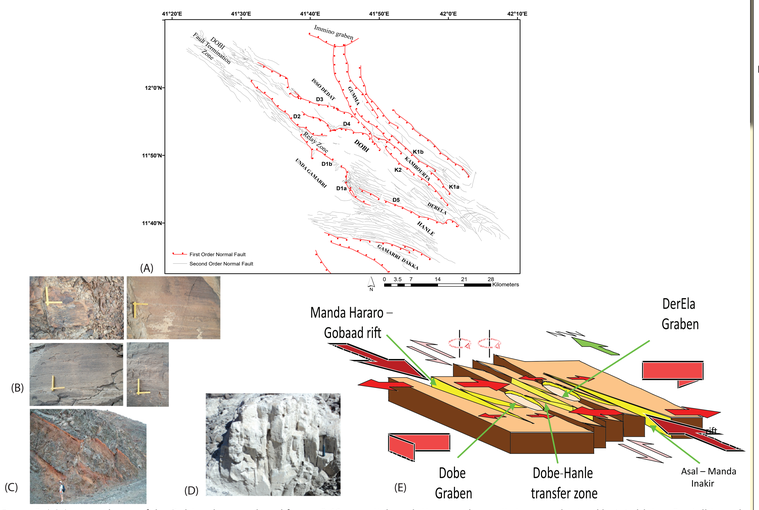

Figure 2. (A) Structural map of the Dobi graben produced from a 0.46 m spatial resolution panchromatic images obtained by Worldview-2 satellite and 1-arc second (30 m) Shuttle Radar Topography Mission (SRTM). (B and C) Normal faulting is dominant, although strike-slip motions along some faults have observed in the field. The Dobi graben's floor is underlain by alluvial and lacustrine sediments, and volcanic. It showed varying colors depending on the degree of weathering ranging from gray to white tones. It has fine to sand grain sizes, slightly weathered and sometimes compacted eolean fans at the foot of the cliffs. (D) The lacustrine sediments mostly composed of the exploitable table salt and associated fine grained sediments having white and dull white colors. Currently the area is being in mined by local people and few investors. (E) Bookshelf model of the East Central Block of the Afar Depression modified after Tapponnier et al. (1990).

Methods and Data

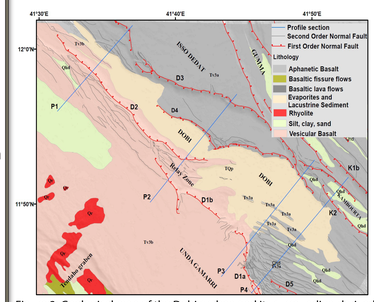

Figure 3: Geological map of the Dobi graben and its surrounding derived from supervised classification of Landsat ETM+ and field geological ground validation.

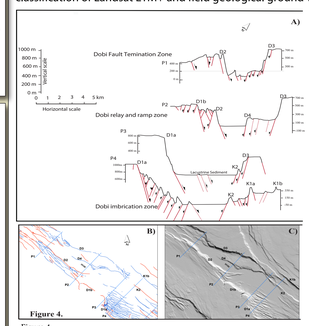

Figure 4.

Figure 4: A) Surface Structural Architecture along N30°E-striking topographic profile P1 to profile P4 across the Dobi graben and Kambourta graben constructed from 1-arc second (30 m) SRTM DEM. Red lines represent the faults, the dashed red lines indicated inferred faults, and small black arrows show slip distributions; B) The apparent dip direction of the faults. The blue lines represent faults dip direction either in the southeast or southwest directions, and the red lines represent the northwest or northeast dip direction of the faults. C) shaded relief map.

RESULTS

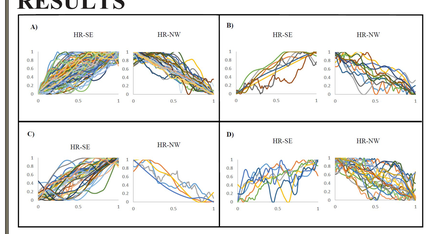

Figure 5: The termination styles and tapering direction of for few samples of the fault in each spatial location is also abbreviated as HR-SE for half restricted and tapering to southeast and HR-NW for half restricted and tapering toward northwest. The X-axis is the normalized failt traced length of the form (l/Lmax) and the y-axis is the normalized fault displacement of the form (D/Dmax).

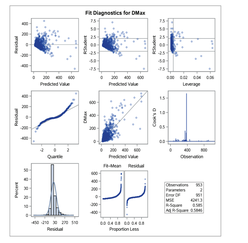

Figure 6: The Statistical analysis revealing the regressional fit diagnostic for Dmax.

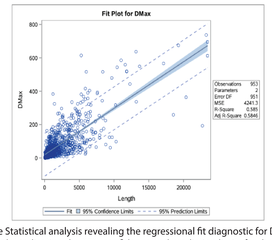

Figure 7: Fit plot indicating the 95% confidence and prediction limits for the 953 normal faults.

RESULTS CONT.

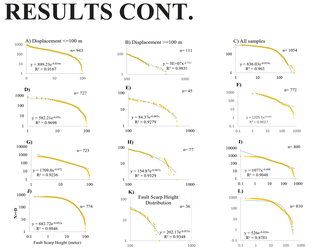

Figure 8.

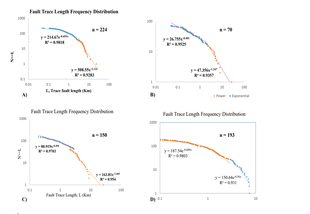

Figure 9.

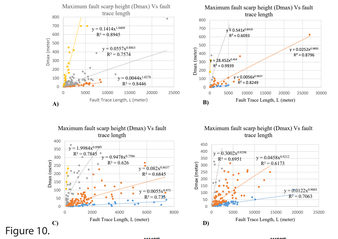

Figure 10.

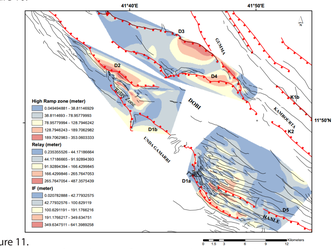

Figure 11.

Figure 8: The log-log frequency distribution of the fault scarps height shows negative exponentials and Power fist A), B) and C) in the Dobi Imbrication Domain; D), E) and F) in the Dobi Relay zone; G), H) and I) in the Dobi High-Linkage Ramp zone; J), K) and L) in the Dobi Fault Termination Zone.
Figure 9: The log-log fault trace length frequency distribution that shows negative exponentials blue color and Power fist orange color A) in the Dobi Imbrication Domain; B) in the Dobi Relay zone; C) in the Dobi High-Linkage Relay zone and; D) in the Dobi Fault Termination Zone.
Figure 10: Normal-Normal Maximum Fault Scarp Height to Fault Trace Length relationships, Orange color represents Constant displacement model, grey color represents Constant Dmax/L ratio, red color represents Increasing Dmax/L ratio and blue color represent Constant Length model color A) in the Dobi Imbrication Domain; B) in the Dobi Relay zone; C) in the Dobi High-Linkage Relay zone and; D) in the Dobi Fault Termination Zone.
Figure 11: The grid displacement gradient map revealed that a higher displacement gradient and elliptical radial shapes (light brown color) found associated with the first order faults that highly localized the stress but have a tendency to diminish toward the center of the graben floor representing stress distribution zone (light blue color).
Figure 12: The structural map of the Dobi graben that are traced in Figure 2 is classified based on the manner on which faults propagations are arrested.
HR is corresponding to a half restricted, TR is stands for tip restricted and UR is for unrestricted.
Figure 13: Structural map showing the different tapering directions of the faults in the Dobi graben and its surrounding.

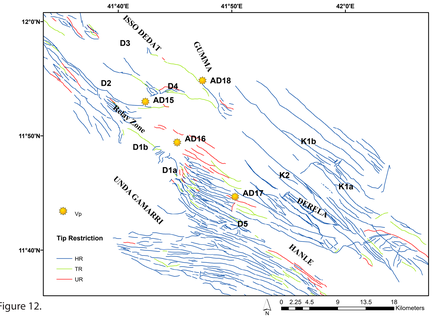

Figure 12.

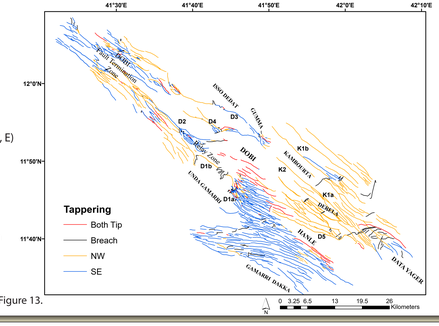

Figure 13.

DISCUSSION

Our analysis of the fault population data suggested that there exist two different types of fault tapering directions in the Dobi graben and its surrounding area, in which ~40% of the fault traced lengths are northwest tapering, and ~45% of the total traced lengths are southeast tapering (Figs. 5 and 13). Additionally, the cumulative traced lengths of faults account for more than 85% of the 953 faults traced in this study resembled the strain directions of either RSR or GAR. For example, Figure 12 and 13 indicate that ~46% of the faults in the Derela fault zone propagate northwest, whereas ~63% of the faults in the Dobi imbrication zone, and Dobi-Hanle fault zone propagate in a southeastern direction. The location of these two oppositely propagating fault systems demonstrates that the northwest tapering is parallel to the southwest tapering faults. Presumably both fault systems taper to zero at the point of contact in the form of a left lateral strike-slip system.

Additionally, a strong correlation between the melt material presence in the lower crust, which was reported by Reed et al. (2014), and the arresting of fault lateral propagation was observed. For example, Figure 12 indicates that lateral propagations are arrested at the four locations indicated by Reed et al. (2014): AD15, AD16, AD17, and AD18. Utilizing a broadband passive seismic receiver function, Reed et al. (2014) reported high Vp/Vs ratios of 1.85 or more within the lower crust beneath the Dobi graben, which implies the presence of melt. Dumont et al. (2016) also suggest that lateral propagation of faults is easier away from areas where magma has been stored for a long time at crustal depth, thus modifying the thermo-mechanical properties of the host rock. The spatial correlation between the melt zones identified by Reed et al. (2014) and the fault lateral propagation arrest shown in this research is presumably due to the thermo-mechanical heterogeneities within the brittle crust which stimulate the initiation of faults. Additionally, they also act as barriers to fault propagation, as demonstrated by the faults labeled D2 and D3 in Figure 2, 4, 12 and 13 as well as many of the intra-rift faults found in the law angle short normal faults located in the Dobi relay, fault termination, and imbrication zones (Figs. 2 and 5; Manighetti et al., 2004, Dumont et al., 2016). In addition, the inelastic deformation due to the highly damaged crust located at the fault tips, as demonstrated in the fault termination zone, is susceptible to preventing the lateral propagation of the faults (Manighetti et al., 2004).

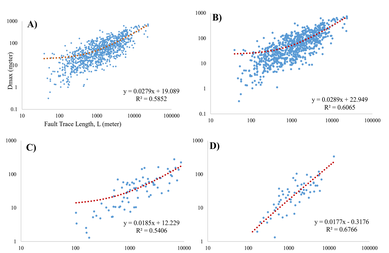

Figure 14: (A) Log-Log plots of Dmax to traced length of all 953 traced faults of the Dobi graben and its surrounding;
(B) Log-Log plots of Dmax to Lmax of those faults that exhibited the termination style of half restricted, HR;
(C) Log-Log plots of Dmax to Lmax of those faults that exhibited the termination style of tip restricted, TR and;
(D) Log-Log plots of Dmax to Lmax of those faults that exhibited unrestricted, UR

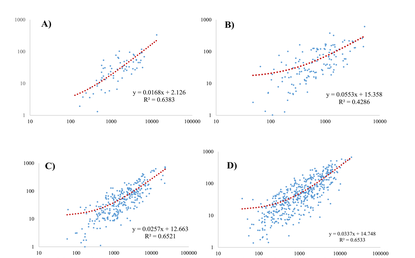

Figure 15. Log-Log plots of Dmax (vertical axis) to traced length (horizontal axis). A) Corresponding to faults that propagating in two opposite directions and tapering at both tips; B) Faults that propagating orthogonal to faults that have a northwest striking direction and considered as a breach; C) Corresponding to faults that tapering in northwest direction and; D) Corresponding to faults that tapering in southeast directions

CONCLUSIONS

- Extension is accommodated by normal faulting and block tilting in the Dobi graben.
- Faults displacement is linearly related to fault length indicating constant growth model.
- Fault propagations is arrested with geological heterogeneities in the graben.
- Regional strain transfer influences the faults tapering directions.

REFERENCE

Demissie, Z.S., Kevin M., Bridges, D., Abdelsalam, M.G., Atekwana, E.A., 2018. Upper lithospheric structure of the Dobi graben, Afar Depression from magnetic and gravity data. Journal of African Earth Sciences. Doi.org/10.1016/j.jafrearsci.2018.06.012

Dumont, S., Socquet, A., Grandin, R., Doubre, C., Klinger, Y., Jacques, E., 2016. Magma influence on propagation of normal faults: Evidence from cumulative slip profiles along Dabbahu-Manda-Hararo rift segment (Afar, Ethiopia). Journal of Structural Geology 95, 48-59.

Reed, C.A., Almadani, S., Gao, S.S., Elsheikh, A.A., Cherie, S., Abdelsalam, M.G., Thurmond, A.K., Liu, K.H., 2014. Receiver function constraints on crustal seismic velocities and partial melting beneath the Red Sea rift and adjacent regions, Afar Depression. J. Geophys. Res.: Solid Earth 119, 2138–2152.

Manighetti, I., King, G., Sammis, C.G., 2004. The role of off-fault damage in the evolution of normal faults. Earth Planet. Sci. Lett. 217 (3), 399e408. Manighetti, I., Campillo, M., Bouley, S., Cotton, F., 2007. Earthquake scaling, fault segmentation, and structural maturity. Earth and Planetary Science Letters 253, 429-438..

Tapponnier, P., Armijo, R., Manighetti, I., and Courtillot, V., 1990, Bookshelf faulting and horizontal block rotations between overlapping rifts in Southern Afar: Geophysical Research Letters, v. 17, no. 1, p. 1-4.